Quantum phase transitions of correlated electrons in two dimensions

Subir Sachdev

Department of Physics, Yale University,
P.O. Box 208120, New Haven, CT 06520-8120, USA.

Abstract

We review the theories of a few quantum phase transitions in two-dimensional correlated electron systems and discuss their application to the cuprate high temperature superconductors. The coupled-ladder antiferromagnet displays a transition between the Néel state and a spin gap paramagnet with a sharp $S = 1$ exciton: we develop a careful argument which eventually establishes that this transition is described by the familiar O(3) φ^4 field theory in 2+1 dimensions. Crucial to this argument is the role played by the quantum Berry phases. We illustrate this role in a one-dimensional example where our results can tested against those known from bosonization. On bipartite lattices in two dimensions, we study the influence of Berry phases on the quantum transition involving the loss of Néel order, and show that they induce bond-centered charge order (*e.g.* spin Peierls order) in the paramagnetic phase. We extend this theory of magnetic transitions in insulators to that between an ordinary d-wave superconductor and one with co-existing spin-density-wave order. Finally, we discuss quantum transitions between superconductors involving changes in the Cooper pair wavefunction, as in a transition between $d_{x^2-y^2}$ and $d_{x^2-y^2} + id_{xy}$ superconductors. A mean-field theory for this transition is provided by the usual BCS theory; however, BCS theory fails near the critical point, and we present the required field-theoretic extension. Our discussion includes a perspective on the phase diagram of the cuprate superconductors, in the context of recent experiments and the transitions discussed here.

Key words: Quantum phase transitions, Berry phases, Néel order, spin gap, bond charge order, superconductivity
PACS: 75.10.Jm, 74.72.-h, 71.27.+a, 71.10.Hf

Email address: subir.sachdev@yale.edu (Subir Sachdev).
URL: http://pantheon.yale.edu/~subir (Subir Sachdev).

1 Introduction

The theory of quantum phase transitions has emerged in the last decade as a powerful tool for the description of the unconventional electronic properties of a variety of correlated systems. This article will provide an elementary overview of some theoretical models of quantum phase transitions in two spatial dimensions, along with a brief discussion of their experimental applications. One reason for our focus on two dimensions is, of course, our interest in the properties of the cuprate superconductors, whose interesting electronic excitations reside within a CuO_2 square lattice. However, not coincidentally, two is also the spatial dimension in which many of the most natural class of non-trivial quantum critical points reside; three is the "upper-critical dimension" of many critical points, at and above which the physical properties are adequately described by a mean field theory (possibly extended with some low order fluctuation corrections).

This article is addressed to newcomers to the study of quantum phase transitions who desire an introduction to some of the experimentally relevant theoretical questions under current discussion. We will assume the reader is well-versed in the standard theory of classical critical phenomena, and so our focus will be on novel aspects of quantum phase transitions, including the role of quantum Berry phases and of excitations with fermionic statistics. Earlier reviews by this author [1,2] provide detailed discussions of background material which we will occasionally refer the reader to; most of our discussion here goes beyond these reviews, and focuses on current theoretical and experimental developments.

We begin in Section 2 by describing the magnetic quantum transition in the coupled ladder antiferromagnet. High precision numerical studies of the critical properties of this transition are now available, and these serve as a useful check on the theoretical models. We map the critical fluctuations of the magnetic Néel order on to the O(3) φ^4 field theory in 2+1 dimensions, along with additional Berry phase terms which reflect the commutation relations of the individual quantum spins. We illustrate the role of the Berry phases by first considering a one-dimensional antiferromagnet in Section 3, where the results can be compared with those obtained by bosonization methods. We return to our discussion of two-dimensional quantum spin models in Section 4, where we extend the methods developed in Section 3: we demonstrate that the Berry phases induce bond-centered charge order in the paramagnetic phase of antiferomagnets with full square lattice symmetry, while they can be safely neglected in the coupled ladder antiferromagnet. The remaining sections extend these theories to doped antiferromagnets with mobile charge carriers. Section 5 considers magnetic transitions in superconductors, while Section 6 describes transitions between BCS superconductors with differing pair wavefunctions.
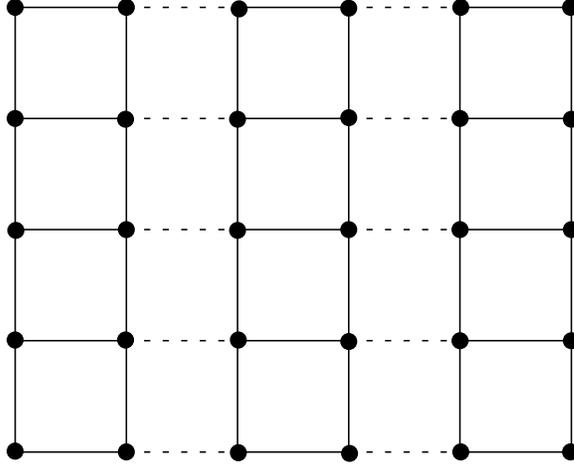
Fig. 1. The coupled ladder antiferromagnet. Spins ($S = 1/2$) are placed on the sites, the A links are shown as full lines, and the B links as dashed lines.

2 Coupled ladder antiferromagnet

We will begin our discussion by describing the quantum phase transition in a simple two-dimensional model of antiferromagnetically coupled $S = 1/2$ Heisenberg spins. At the microscopic level, this model does not describe the spin fluctuations in the cuprate superconductors. However, a fairly subtle argument, which we develop in the following sections and culminate in Section 5, shows that the universal properties of the simple critical point described in this section are identical to those of a magnetic ordering transition in the cuprate superconductors. The model presented here also provides a useful description of other transition metal oxides with a spin gap [3].

We consider the "ladder" Hamiltonian

$$H_\ell = J \sum_{i,j \in A} \mathbf{S}_i \cdot \mathbf{S}_j + \lambda J \sum_{i,j \in B} \mathbf{S}_i \cdot \mathbf{S}_j \tag{1}$$

where $\mathbf{S}_i$ are spin-1/2 operators on the sites of the coupled-ladder lattice shown in Fig 1, with the A links forming decoupled two-leg ladders while the B links couple the ladders as shown. The ground state of H depends only on the dimensionless coupling λ, and we will describe the low temperature properties as a function of λ. We will restrict our attention to $J > 0$ and $0 \leq \lambda \leq 1$.

We will begin with a physical discussion of the phases and excitations of the coupled ladder antiferromagnet, H_ℓ in Section 2.1. We will propose a quantum field-theoretical description of this model in Section 2.2: we will verify that the limiting regimes of the field theory contain excitations whose quantum numbers numbers are in accord with the phases discussed in Section 2.1, and will then use the field theory to describe the critical point.
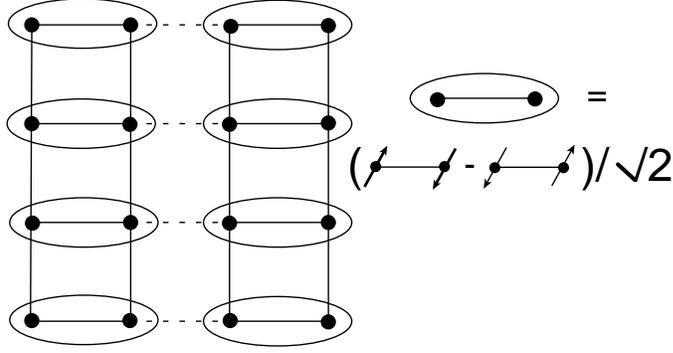
Fig. 2. Schematic of the quantum paramagnet ground state for small λ. The ovals represent singlet valence bond pairs.

2.1   Phases and their excitations

Let us first consider the case where λ is close to 1. Exactly at $\lambda = 1$, H is identical to the square lattice Heisenberg antiferromagnet, and this is known to have long-range, magnetic Néel order in its ground state *i.e.* the spin-rotation symmetry is broken and the spins have a non-zero, staggered, expectation value in the ground state with

$$\langle \mathbf{S}_j \rangle = \eta_j N_0 \mathbf{n}, \tag{2}$$

where $\mathbf{n}$ is some fixed unit vector in spin space, and η_j is ± 1 on the two sublattices. This long-range order is expected to be preserved for a finite range of λ close to 1. The low-lying excitations above the ground state consist of slow spatial deformations in the orientation $\mathbf{n}$: these are the familiar spin waves, and they can carry arbitrarily low energy *i.e.* the phase is 'gapless'. There are *two* polarizations of spin waves at each wavevector $k = (k_x, k_y)$ (measured from the antiferromagnetic ordering wavevector), and they have excitation energy $\varepsilon_k = (c_x^2 k_x^2 + c_y^2 k_y^2)^{1/2}$, with c_x, c_y the spin-wave velocities in the two spatial directions.

Let us turn now to the vicinity of $\lambda = 0$. Exactly at $\lambda = 0$, H is the Hamiltonian of a set of decoupled spin ladders. Such spin ladders are known to have a paramagnetic ground state, with spin rotation symmetry preserved, and an energy gap to all excitations [4]. A caricature of the ground state is sketched in Fig 2: spins on opposite rungs of the ladder pair in valence bond singlets in a manner which preserves all lattice symmetries. Excitations are now formed by breaking a valence bond, which leads to a *three*-fold degenerate state with total spin $S = 1$, as shown in Fig 3; this broken bond can hop from site-to-site, leading to a triplet quasiparticle excitation. Note that this quasiparticle is *not* a spin-wave (or equivalently, a 'magnon') but is more properly referred to as a spin 1 *exciton*. For λ small, but not exactly 0, we expect that the ground
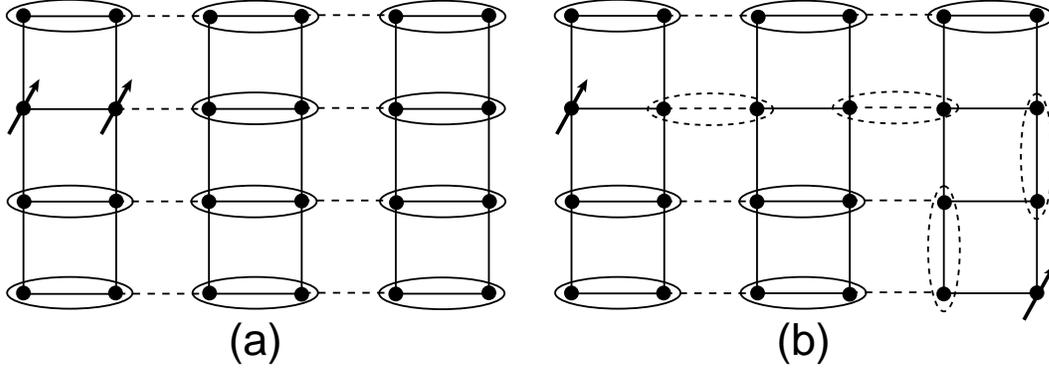
Fig. 3. (a) Cartoon picture of the bosonic $S = 1$ exciton of the paramagnet. (b) Fission of the $S = 1$ excitation into two $S = 1/2$ spinons. The spinons are connected by a "string" of valence bonds (denoted by dashed ovals) which are not able to resonate with their environment, and some of which lie on weaker bonds; this string costs a finite energy per unit length and leads to the confinement of spinons.

state will remain a gapped paramagnet, and the spin exciton will now move in two dimensions. We parameterize its energy at small wavevectors by

$$\varepsilon_k = \Delta + \frac{c_x^2 k_x^2 + c_y^2 k_y^2}{2\Delta}, \tag{3}$$

where Δ is the spin gap, and c_x, c_y are velocities. Fig 3 also presents a simple argument which shows that the $S = 1$ exciton cannot fission into two $S = 1/2$ 'spinons'.

The very distinct symmetry signatures of the ground states and excitations between $\lambda \approx 1$ and $\lambda \approx 0$ make it clear that the two limits cannot be continuously connected. It is known [5,6] that there is an intermediate second-order phase transition at $\lambda = \lambda_c \approx 0.3$. Both the spin gap Δ and the Néel order parameter N_0 vanish continuously as λ_c is approached from either side.

2.2 Quantum field theory

A convenient field-theoretic description of the two phases introduced in Section 2.1, and of the critical point which separates them, is obtained by the coherent state path integral. A detailed derivation of this approach has been provided by the author in Chapter 13 of Ref. [1] which the reader should now consult; we will only highlight a few important points here.

The coherent state path integral is best introduced by considering first a single spin $\mathbf{S}$ with angular momentum S and Hamiltonian

$$H_0 = -\mathbf{h} \cdot \mathbf{S} \tag{4}$$

where $\mathbf{h}$ is a static magnetic field. The $(2S+1)$ eigenvalues of H_0 are, of course, $-m|\mathbf{h}|$, where $m = -S, -S+1, \ldots, S-1, S$, and so we also know its partition function Z_0 at a temperature T. The coherent state path integral represents Z_0 in terms of an integral over all possible closed curves, $\mathbf{N}(\tau)$, on the surface of a unit sphere, each curve representing a possible history of the precessing spin in imaginary time, τ:

$$Z_0 = \int \mathcal{D}\mathbf{N}(\tau)\delta(\mathbf{N}^2(\tau) - 1) \exp\left(-iS \int \mathcal{A}_\tau(\mathbf{N}(\tau))d\tau + \int d\tau S\mathbf{h} \cdot \mathbf{N}(\tau)\right). \quad (5)$$

The first term is the so-called 'Berry phase', and $\mathcal{A}_\tau(\mathbf{N}(\tau))d\tau$ is defined to be the oriented area of the spherical triangle defined by $\mathbf{N}(\tau)$, $\mathbf{N}(\tau + d\tau)$, and an arbitrary reference point $\mathbf{N}_0$ (which is usually chosen to be the north pole). We will see that $\mathcal{A}_\tau$ behaves in many respects like the time-component of a gauge field, and this accounts for the suggestive notation. All physical results should be independent of the choice of $\mathbf{N}_0$, and it is easy to see that changes in $\mathbf{N}_0$ amount to gauge transformations of $\mathcal{A}_\tau$. So if we change $\mathbf{N}_0$ to $\mathbf{N}_0'$, then the resulting $\mathcal{A}_\tau'$ is related to $\mathcal{A}_\tau$ by

$$\mathcal{A}_\tau' = \mathcal{A}_\tau - \partial_\tau \phi(\tau) \quad (6)$$

where $\phi(\tau)$ measures the oriented area of the spherical triangle defined by $\mathbf{N}(\tau)$, $\mathbf{N}_0$, and $\mathbf{N}_0'$.

We now apply the above path integral independently to every site of the coupled ladder antiferromagnet: we obtain a path integral over fields $\mathbf{N}_j(\tau)$, where j is a site index as in (1). As discussed in Chapter 13 of Ref. [1], it is convenient to now take a spatial continuum limit, to allow focus on the important low energy excitations. This proceeds by the parameterization

$$\mathbf{N}_j(\tau) = \eta_j \mathbf{n}(r_j, \tau)\sqrt{1 - (a^2/S)^2 \mathbf{L}^2(r_j, \tau)} + \frac{a^2}{S}\mathbf{L}(r_j, \tau), \quad (7)$$

where $\eta_j = \pm 1$ on the two subattices, a is the lattice spacing, $r \equiv (x, y)$, $\mathbf{n}(r, \tau)$ is a unit length continuum field representing the staggered Néel order parameter, and $\mathbf{L}(r, \tau)$ is the continuum field for the conserved, uniform, magnetization density (the normalization chosen in (7) is that required to make $\int d^2r\mathbf{L}(r, \tau)$ exactly equal to the total spin). Next, a gradient expansion in performed on the effective action for H_ℓ, and after integrating out the $\mathbf{L}$ fluctuations we obtain the following path integral for the partition function of the coupled ladder antiferromagnet:

$$Z_\ell = \int \mathcal{D}\mathbf{n}(r, \tau)\delta(\mathbf{n}^2(r, \tau) - 1) \exp\left[-iS\sum_j \eta_j \int d\tau \mathcal{A}_\tau(\mathbf{n}(r_j, \tau))\right.$$

$$-\frac{1}{2g\sqrt{c_x c_y}} \int d^2r d\tau \left((\partial_\tau \mathbf{n})^2 + c_x^2 (\partial_x \mathbf{n})^2 + c_y^2 (\partial_y \mathbf{n})^2\right)\right], \quad (8)$$

where the velocities $c_x = JSa\sqrt{(1+\lambda)(3+\lambda)}$, $c_y = JSa\sqrt{2(3+\lambda)}$, and the coupling constant $g = (2a/S)[(3+\lambda)^2/(2+2\lambda)]^{1/4}$. We will now view g as the tuning parameter, and values of g on either side of a critical value g_c place the system in one of the two phases discussed in Section 2.1; notice that g is a decreasing function of λ for $0 < \lambda < 1$, and so the "strong" coupling phase $g > g_c$ corresponds to the spin gap phase with $\lambda < \lambda_c$, while $g < g_c$ is the $\lambda > \lambda_c$ Néel phase.

The first term in (8) is a residual Berry phase, and this remains expressed on the underlying lattice: there is no natural way to take its continuum limit. Notice that this term induces complex weights in the partition function and so it has no analog in the theory of classical phase transitions. This Berry phase plays a central role in determining the phases and critical points of many quantum spin systems, and describing its consequences is one of the central purposes of this article. However, our discussions in the following sections will show that at least for the case of the coupled ladder antiferromagnet the Berry phase in (8) can be safely neglected, and so we will drop it in the remainder of this subsection.

Upon omission of the Berry phase in (8), Z_ℓ becomes a standard path integral, familiar in well established theories of classical phase transitions in $3 = 2 + 1$ dimensions. For instance, after interpreting τ as a third dimension (*i.e.* $\tau \to z$), and $\mathbf{n}$ as the local magnetization in a three-dimensional ferromagnet (*e.g.* iron), then Z_ℓ is simply its *classical* partition function at a finite 'temperature' T_{cl}, with the coupling constant $g \sim T_{cl}$. From the theory of such ferromagnets it is known that a convenient description of the physical properties of Z_ℓ emerges not in a formulation in terms of the fixed length field $\mathbf{n}$ (the 'hard spin' representation), but in a formulation using a 'soft spin' field $\varphi_\alpha(r, \tau)$ ($\alpha = x, y, z$) with no length constraint. We connect the two formulations by a coarse-graining transformation, so that φ_α represents the average of $\mathbf{n}$ over some small coarse-graining volume of spacetime. The new form of Z_ℓ is now

$$Z_\ell = \int \mathcal{D}\varphi_\alpha(r,\tau) \exp\left[-\int d^2r d\tau \left\{\frac{1}{2}\left((\partial_\tau \varphi_\alpha)^2 + c_x^2 (\partial_x \varphi_\alpha)^2 + c_y^2 (\partial_y \varphi_\alpha)^2\right.\right.\right.$$
$$\left.\left.\left. +s\varphi_\alpha^2\right) + \frac{u}{24}\left(\varphi_\alpha^2\right)^2\right\}\right], \quad (9)$$

where keep in mind that the Berry phase in (8) has been dropped, s is now the new tuning parameter (replacing g in (8)), and the quartic interaction u has replaced the fixed length constraint in (8). The two phases of Section 2.1

are now separated by a critical value $s = s_c$, with the $\lambda < \lambda_c$ spin gap phase corresponding to $s > s_c$, while the $\lambda > \lambda_c$ Néel phase appears for $s < s_c$.

The well-known properties of the model (9), when translated into the quantum framework of interest here, are easily seen to reproduce the physical properties of the phases discussed in Section 2.1.

For $s < s_c$, Z_ℓ in (9) has a "ferromagnetic" phase associated with the breaking of spin rotation invariance, and the development of the expectation value $\langle \varphi_\alpha \rangle = \delta_{\alpha z} N_0$; to lowest order in u, the spontaneous magnetization is $N_0 = \sqrt{-6s/u}$ and is determined by the minimum of the "Mexican hat" potential for the φ_α field. After using (7) this "ferromagnetic" order in the classical model is seen to correspond to the antiferromagnetic Néel order (2) in the quantum model. A standard Gaussian fluctuation analysis about this ordered states shows that susceptiblity transverse to the spontaneous moment is given by

$$\chi_\perp(k, \omega_n) = \left\langle |\varphi_x(k, \omega_n)|^2 \right\rangle = \left\langle |\varphi_y(k, \omega_n)|^2 \right\rangle = \frac{1}{\omega_n^2 + c_x^2 k_x^2 + c_y k_y^2} \tag{10}$$

where ω_n is a frequency associated with imaginary time. After analytically continuing to real frequencies, ω, this yields the quantum response function to an applied staggered field transverse to the Néel order:

$$\chi_\perp(k, \omega) = \frac{1}{c_x^2 k_x^2 + c_y k_y^2 - \omega^2}. \tag{11}$$

This response function has a pole, representing the two spin-wave excitations, at energy $\left(c_x^2 k_x^2 + c_y^2 k_y^2 \right)^{1/2}$. This is in complete accord with our discussion of the properties of the Néel phase in Section 2.1.

For $s > s_c$, the "disordered" phase of Z_ℓ in (9) corresponds to the quantum paramagnet with a spin gap. Here, a computation of the susceptibility to lowest order in u yields

$$\chi(k, \omega) = \frac{\mathcal{Z}}{\Delta^2 + c_x^2 k_x^2 + c_y k_y^2 - \omega^2}, \tag{12}$$

where we have already analytically continued to real frequencies, $\Delta = \sqrt{s}$, and (for now) the residue $\mathcal{Z} = 1$. This response function is independent of the direction of the applied staggered field, and so its pole represents the $S = 1$ exciton at energy $\left(\Delta^2 + c_x^2 k_x^2 + c_y^2 k_y^2 \right)^{1/2}$. This is again in accord with the discussion of the spin gap phase in Section 2.1: the exciton dispersion (3) is obtained from the present result in a small momentum expansion. The

8

pole structure in (12) actually holds to all orders in an expansion in u [1]: at quantum temperature $T = 0$, such corrections renormalize the values of the spin gap Δ and the quasiparticle residue $\mathcal{Z}$, and induce additional spectral weight associated with multiple excitonic continua at energies larger than 3Δ, but they do not broaden the quasiparticle pole. Physically, this happens because the exciton is the lowest energy excitation with spin $S = 1$, and so conservation of total spin prevents implies that this excitation has an infinite lifetime. Only at $T > 0$ does a finite lifetime appear, associated with scattering off the thermally excited density of pre-exiting excitons.

The present field theoretical framework can also be extended to obtain a theory for the critical point at $s = s_c$ ($\lambda = \lambda_c$), as has been discussed in some detail in [1]. In its application to the classical ferromagnet, the critical properties of (9) have been understood in some detail in studies of the φ^4 field theory, and accurate values of the critical exponents have been obtained. In a recent quantum Monte Carlo study of the coupled ladder antiferromagnet H_ℓ, Matsumoto *et al.* [7] determined the critical exponents at $\lambda = \lambda_c$ to impressive accuracy, and all values are in accord with the exponents of the φ^4 field theory. This agreement is independent numerical support for the omission of the Berry phases in proceeding from (8) to (9); separate theoretical arguments for the same approximation will emerge in the following sections. As we approach the critical point with $s \searrow s_c$, the pole structure in (12) continues to hold at low frequencies, but the spin gap vanishes as $\Delta \sim (s - s_c)^{z\nu}$ and the residue vanishes as $\mathcal{Z} \sim (s - s_c)^{\eta\nu}$, where $z = 1$, ν, and η are standard critical exponents. Right at $s = s_c$ there are no quasiparticle excitions, and the dynamic susceptiblity instead displays a branch-cut representing the continuum of critical excitations:

$$\chi(k, \omega) \sim \frac{1}{\left(c_x^2 k_x^2 + c_y^2 k_y^2 - \omega^2\right)^{1-\eta/2}}. \tag{13}$$

For more information on the physics of this critical continuum, refer to [1].

3   Quantum XY chain

This section will divert from the main subject of this paper by considering some simple examples of quantum phase transitions in one dimension. Our purpose here is to illustrate the consequences of the Berry phases in (8) by considering a simplified model for which they can be evaluated completely; we will also be able to test our method by comparing the results with those obtained by a bosonization analysis of the same one-dimensional model. We will then proceed to apply closely related methods in two dimensions in Section 4.

9

We will evaluate the generalization of (8) in one dimension for case in which the Hamiltonian has on a global U(1) spin symmetry, and the anisotropies are such that the spins prefer to lie within the x-y plane in spin space. In this case we can parameterize $\mathbf{n}$ by a single angle θ:

$$\mathbf{n} = (\cos\theta, \sin\theta, 0); \tag{14}$$

with these simplifications, we will find that powerful duality methods enable us to obtain considerable insight into the physics a partition function with Berry phases and complex weights. With the parameterization (14) and the restriction to one spatial dimension, we expect the resulting Z_ℓ to provide a description of a large class of spin S quantum antiferromagnets in one dimension; to be specfic, we expect it will model the Hamiltonian

$$H_{XY} = J_1 \sum_j \left(S_{xj} S_{x,j+1} + S_{yj} S_{y,j+1} + \zeta S_{zj} S_{z,j+1} \right)$$
$$+ J_2 \sum_j \left(S_{xj} S_{x,j+2} + S_{yj} S_{y,j+2} + \zeta S_{zj} S_{z,j+2} \right), \tag{15}$$

where $J_{1,2} > 0$ are first/second neighbor antiferromagnetic exchange constants (J_2 is not too large), and the anisotropy $|\zeta| < 1$ induces a preference for the spins to reside in the x-y plane. We can reasonably expect that the phase diagram of H_{XY} as a function of ζ and J_2/J_1 is similar to that of Z_ℓ as a function of g. The former is already known by an earlier bosonization analysis [9] and will provide an instructive comparison with the latter.

Our computation begins by a transformation of the Berry phase in (8) to an alternative form in one dimension. We discretize spacetime into a square lattice of sites, j, (j is now a spacetime index, unlike the spatial index in (15), and its interpretation should be clear from the context). For this spacetime lattice we define $\mathcal{A}_{j\mu}$, with $\mu = x, \tau$, to be the oriented area of the spherical triangle formed by $\mathbf{n}_j$, $\mathbf{n}_{j+\hat{\mu}}$, and a fixed reference $\mathbf{N}_0$. Then, as illustrated in Fig 4, we can use the identity

$$\sum_j \eta_j \mathcal{A}_{j\tau} = \sum_j \ell_{\bar{j}} \epsilon_{\mu\nu} \Delta_\mu \mathcal{A}_{j\nu} \tag{16}$$

to relate the Berry phase to the $\mathcal{A}_\mu$ flux piercing the plaquettes of the spacetime lattice; here $\ell_{\bar{j}}$ is a fixed integer field on the sites, $\bar{j}$, of the dual lattice, and a convenient choice is $\ell_{\bar{j}} = (1 - (-1)^{\bar{j}_x})/2$ *i.e.* $\ell_{\bar{j}}$ is unity on every odd column, and zero on every even column. The symbol Δ_μ represents a discrete lattice derivative, with $\Delta_\mu f_j \equiv f_{j+\hat{\mu}} - f_j$.

Now we use the in-plane form of $\mathbf{n}$ in (14) to our advantage. The flux $\epsilon_{\mu\nu} \Delta_\mu \mathcal{A}_{j\nu}$ through any plaquette is clearly equal to the surface area of the quadrilateral
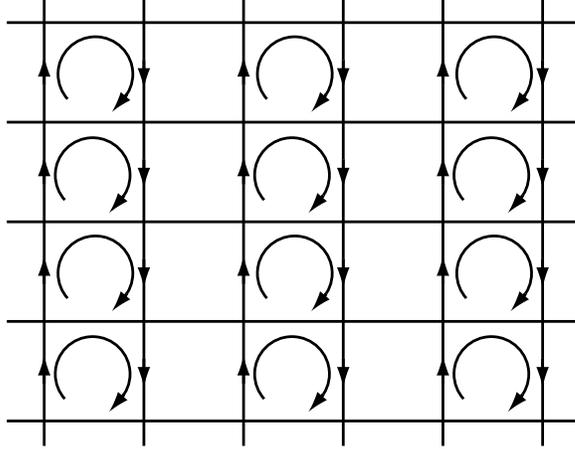
Fig. 4. Diagrammatic proof of the identity (16) which relates the Berry phase to the sum over the $\mathcal{A}_\mu$ flux in every plaquette in the odd columns.

on the unit sphere formed by the $\mathbf{n}_j$ on the four vertices of the plaquette. For planar spins, such a quadrilateral lies entirely on the equator, and its area is generically zero. The only exception occurs when a vortex in θ pierces the plaquette: in this case, the quadrilateral is the entire equator and the flux is the area of a hemisphere $= \pm 2\pi$. So we have established that the Berry phases in (8) generate the factor

$$\exp\left(-i2\pi S \sum_{\bar{j}} \ell_{\bar{j}} \times (\text{vortex number of plaquette } \bar{j})\right) \qquad (17)$$

for easy-plane spin systems in one dimension. As the vortex number is always an integer, we see that the factor in (17) is always unity for integer S, and the Berry phases can be ignored for these values of S.

The remaining terms in the action of (8) can also be simplified for the present situation. On the discrete spacetime lattice, and with (14), these terms become $-(1/g) \sum_j \cos(\Delta_\mu \theta_j)$, which is the usual action of a "classical" XY model in $2 = 1 + 1$ dimensions. As is standard, duality manipulations on this XY model are more conveniently performed in a periodic Gaussian, 'Villain', representation of the weights of the model. In this manner, we finally obtain the generalization of the partition function (8) to U(1) symmetric, quantum spin S chains:

$$Z_{XY} = \sum_{\{m_{j\mu}\}} \int \prod_j d\theta_j \exp\left(-\frac{1}{2g}\sum_{j\mu}(\Delta_\mu\theta_j - 2\pi m_{j\mu})^2 - i2\pi S \sum_{\square}\epsilon_{\mu\nu}\ell_{\bar{j}}\Delta_\mu m_{j\nu}\right), (18)$$

where $m_{j\mu}$ are integers on the links of the direct lattice which, when summed, produce the periodic Gaussian weights for $\Delta_\mu \theta_j$, the $\square$ represents a sum over

11

plaquettes, and $\epsilon_{\mu\nu}\Delta_\mu m_{j\nu}$ are the vortex numbers of the plaquettes. The expression (18) is amenable to an exact duality transformation which produces a representation in which all weights are positive: we apply the Poisson summation identity to the sum over $m_{j\mu}$ on each link, and replace it by a sum over integers $J_{j\mu}$:

$$Z_{XY} = \sum_{\{J_{j\mu}\}} \int \prod_j d\theta_j \exp\left(-\frac{g}{2}\sum_{j\mu}(J_{j\mu} - S\epsilon_{\mu\nu}\Delta_\nu\ell_{\bar{j}})^2 - i\sum_{j\mu}J_{j\mu}\Delta_\mu\theta_j\right). \quad (19)$$

Here, and henceforth, we drop overall normalization constants in front of partition functions. Now the integral over the θ_j can be performed independently on each site, and only imposes the constraint $\Delta_\mu J_{j\mu} = 0$. We solve this constraint by writing $J_{j\mu} = \epsilon_{\mu\nu}\Delta_\nu p_{\bar{j}}$, with the $p_{\bar{j}}$ integers on the sites of the dual lattice. So we obtain the exact mapping of (18) to [8]

$$Z_{XY} = \sum_{\{H_{\bar{j}}\}} \exp\left(-\frac{g}{2}\sum_{\bar{j}}(\Delta_\mu H_{\bar{j}})^2\right), \quad (20)$$

where the "heights" $H_{\bar{j}}$ on the sites of the dual lattice are restricted to the values

$$H_{\bar{j}} \equiv p_{\bar{j}} - S\ell_{\bar{j}} \quad (21)$$

The expression (20) is a canonical height (or 'solid-on-solid') model in two dimensions. The only influence of the quantum Berry phase are the restrictions on the allowed values of the heights of the "interface": for integer S the heights take all integer values just as in the standard solid-on-solid model, while for half-integer S, the heights are restricted to half-odd-integer (integer) values on the odd (even) columns of the square lattice. As we have made a number of approximations in the deriving Z_{XY} from the path integral of spin systems, we shall be interested in a generalized class of height models with additional short-range non-local couplings, apart from the simple terms appearing in (20). With these additional couplings, standard methods from the theory of interface models can be used to show [8] that the generalized height models describe phases not only in the easy-plane, small $|\zeta|$, limit of (15), but also those in the easy-axis, large $|\zeta|$ limit when the spins prefer to lie in the $\pm z$ directions. In all of this analysis it is essential that we not relax the restrictions on the allowed values of the heights, as these are fundamental consequences of the quantized value of the spin S. We describe the main results for two sets of S values in turn.

3.1 S integer

The standard model with integer heights on every site has two phases. For small g, the interface is rough; this is dual to the classical or quantum XY phase with quasi-long-range spin order in the x-y plane, with power-law decay of spin correlations. For the quantum spin chain, we may refer to this phase as a Tomonaga-Luttinger (TL) liquid, as it shares many of the characteristics of other TL liquids.

For large g, the interface is smooth; this is dual to the "disordered" phase of the classical XY model. For the quantum spin chain, this large g phase has exponential decay of spin correlations in imaginary time, and therefore a spin gap. Its characteristics are rather similar to the spin gap phase discussed in Section 2: the primary excitation is a gapped $S = 1$ exciton with an infinite lifetime at low energies. As the spin anisotropy is reduced by increasing ζ in (15), this spin gap phase connects continuously to the well-known Haldane gap state of integer spin chains with SU(2) symmetry.

The transition between the small and large g phases is second-order, and is described by the standard Kosterlitz-Thouless theory of the classical XY model in two dimensions.

3.2 S half-odd-integer

The staggering of the heights between integer and half-odd-integer values introduces crucial differences in the phase diagram, and several new phases are allowed in the generalized phase diagram of such height models. However, it is believed [8] that the specific height model (20), with only a local gradient squared coupling, has only one rough phase for all values of g, and this corresponds, as above, to a TL phase of the quantum spin chain. The other phases appear upon allowing additional short-range couplings in (20), and these can reasonably be expected to arise from terms in the original Hamiltonian omitted in the duality mappings; as we noted above, in this generalization it is essential that we maintain the restrictions on the allowed height values. The new phases are associated with smooth interfaces, and as in (3.1 such phases have a spin gap. However, the staggering of the heights induces crucial differences in the structure of such spin gap states, as we describe below.

A crucial characteristic of a smooth interface is that there is a well-defined value of the average height $\langle H_{\bar{\jmath}} \rangle$ in every pure state. Furthermore, for the staggered height models under consideration here, every value of the average $\langle H_{\bar{\jmath}} \rangle$ *breaks a lattice translational symmetry of the quantum spin chain.* For instance if $\langle H_{\bar{\jmath}} \rangle = 0$ (modulo integers) then the even columns of the square
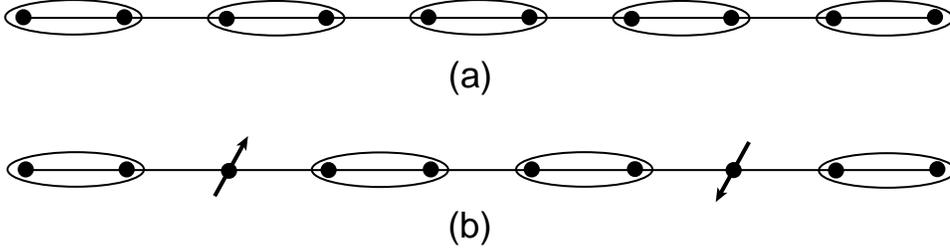
Fig. 5. (a) Schematic of the state with bond-centered charge (BC) or spin-Peierls order for the $S = 1/2$ quantum spin chain. The ellipses represent valence bonds as in Fig 2, and these have spontaneously chosen one of two possible dimerizations of the chain. (b) $S = 1/2$ spin excitations of the BC state. Unlike the case in Fig 3b, these spinons are free to move far apart from each other: this is because we are in one dimension *and* the dimerization is spontaneous. Such spinons are confined in two dimensions whether the BC order is spontaneous or explicitly present in the Hamiltonian.

lattice (which have integer allowed heights) have been picked out, and we may expect the average energy, $\langle S_{jx}S_{j+1,x} + S_{jy}S_{j+1,y} \rangle$ on the links associated with the even columns to be smaller (say) than those on the odd columns. Conversely, an interface with $\langle H_{\bar{j}} \rangle = 1/2$ (modulo integers) reverses the role of the odd and even columns. The choice between these two sets of average heights corresponds to a spontaneously broken Z_2 symmetry in the ground state, which now has 'spin-Peierls' or 'bond-centered charge' (BC) order. The nature of these ordered states, and of their excitations, is illustrated in Fig 5: they have a spin gap, but the lowest-lying excitations are fractionalized $S = 1/2$ spinons which reside on the domain wall between the two BC states.

Other possible values of $\langle H_{\bar{j}} \rangle$ in the smooth interface phase lead to other discrete broken symmetries in the quantum spin chain. As we describe in Ref. [8], the values $\langle H_{\bar{j}} \rangle = 1/4, 3/4$ (modulo integers) correspond to states with Ising spin order *i.e.* $\langle S_{jz} \rangle = \pm\eta_j N_0$. All other values of $\langle H_{\bar{j}} \rangle$ correspond to four-fold degenerate states with co-existing Ising and BC order.

We sketch the phase diagram of the model (20) for S half-odd-integer in Fig 6, as obtained by a bosonization analysis [9]. The TL, BC, and Ising phases are all separated by second-order transition lines, and the three lines meet at a single multi-critical point: all the critical properties can be described by an extension of the Kosterlitz-Thouless renormalization group flows. Analysis of the generalized height models discussed here leads to a phase diagram with an identical topology and critical properties [8].
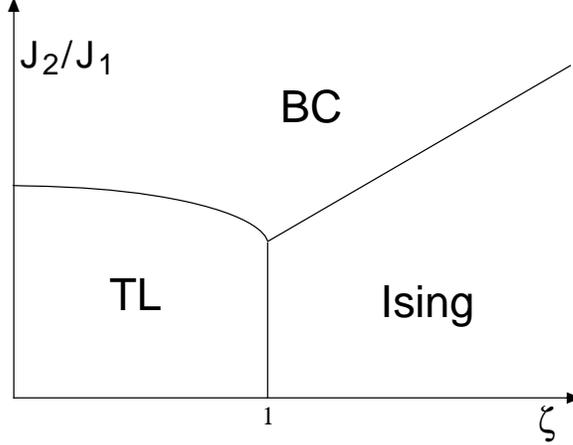
Fig. 6. Phase diagram of the $S = 1/2$ quantum spin chain H_{XY} as obtained by abelian bosonization [9]. Identical results are obtained from a generalized square lattice height model in which the heights take half-odd-integer (integer) values on the even (odd) columns.

4 Berry phases in two dimensions

We are now prepared to describe the evaluation of the 2+1 dimensional path integral with Berry phases in (8). As in the 1+1 dimensional case in Section 3 the evaluation is performed on a discrete lattice in spacetime: the degrees of freedom are three component unit vectors, $\mathbf{n}_j$, on the sites, j of a cubic lattice. On such a lattice we can rewrite (8) as

$$Z = \int \prod_j d\mathbf{n}_j \delta(\mathbf{n}_j^2 - 1) \exp\left(-\frac{1}{2g}\sum_{j,\mu} \mathbf{n}_j \cdot \mathbf{n}_{j+\hat{\mu}} - iS\sum_j \eta_j \mathcal{A}_{j\tau}\right), \qquad (22)$$

where the sum over μ extends over the three directions x,y,τ. In the application to the coupled latter antiferromagnet, the spatial anisotropy and doubled unit cell of H_ℓ led to an anisotropy in the spatial derivative terms in (8). In the discrete form (22) this reduced symmetry requires a corresponding variation in the couplings g associated with the couplings between the various sites on the cubic spacetime lattice: we have dropped this variation in (22) and so, strictly speaking, this partition function applies only to quantum antiferromagnets which have the full symmetry of the square lattice and have a single spin S on each site. An example of such an antiferromagnet is the so-called J_1-J_2 model

$$H = J_1 \sum_{\langle ij \rangle} \mathbf{S}_i \cdot \mathbf{S}_j + J_2 \sum_{\text{nnn } ij} \mathbf{S}_i \cdot \mathbf{S}_j \qquad (23)$$

with exchange interaction $J_1 > 0$ between square lattice nearest neighbors $\langle ij \rangle$, and $J_2 > 0$ between next-nearest-neighbors (nnn). As in Section 3, we

15

exclude large values of J_2 and expect that the phases of H as a function of J_2/J_1 will be described by those of Z in (22) as a function of g. Later we will also discuss the consequences of doubling the unit cell and introducing spatial anisotropy in (22), which is required to obtain a description of the coupled ladder model in (1).

For small g, we expect Z to be in the ordered Néel state, with broken spin rotation symmetry. It is not difficult to account for the Berry phases in a spin-wave fluctuation analysis about this ordered state, and they only have minor consequences [8].

The Berry phases are more crucial in the paramagnet state, with full spin rotation symmetry, expected at large g. Because this is a strongly coupled system in the 3 dimensions with a non-abelian symmetry, no exact duality analysis is possible (unlike the simpler situation in Section 3). We proceed with the strategy discussed in Ref. [8]: we replace the integral over the $\mathbf{n}_j$ by an integral over the $\mathcal{A}_{j\mu}$ the variables that appear in the Berry phases. Formally, this can be done by introducing new 'dummy' variables $A_{j\mu}$ and rewriting (22) by introducing factors of unity on each link; this leads to

$$
Z = \int \prod_{j\mu} dA_{j\mu} \exp\left(-iS\sum_j \eta_j A_{j\tau}\right) \int \prod_j d\mathbf{n}_j \delta(\mathbf{n}_j^2 - 1)\delta(\mathcal{A}_{j\mu} - A_{j\mu})
$$

$$
\times \exp\left(-\frac{1}{2g}\sum_{j,\mu} \mathbf{n}_j \cdot \mathbf{n}_{j+\hat{\mu}}\right)
$$

$$
= \int \prod_{j\mu} dA_{j\mu} \exp\left(-\mathcal{S}_A(A_{j\mu}) - iS\sum_j \eta_j A_{j\tau}\right). \tag{24}
$$

In the first expression, if the integral over the $A_{j\mu}$ is performed first, we trivially return to (22); however in the second expression we perform the integral over the $\mathbf{n}_j$ variables first at the cost of introducing an unknown effective action $\mathcal{S}_A$ for the $A_{j\mu}$. In principle, evaluation of $\mathcal{S}_A$ may be performed order-by-order in a "high temperature" expansion in $1/g$: we match correlators of the $A_{j\mu}$ flux with those of the $\mathcal{A}_{j\mu}$ flux evaluated in the integral over the $\mathbf{n}_j$ with positive weights determined only by the $1/g$ term in (22). Rather than undertaking this laborious calculation, we can guess essential features of the effective action $\mathcal{S}_A$ from some general constraints. First, correlations in the $\mathbf{n}_j$ decay exponentially rapidly for large g (with a correlation length $\sim 1/\ln(g)$), and so $\mathcal{S}_A$ should be local. Second, it should invariant under the lattice form of the gauge transformation (6)

$$
A'_{j\mu} = A_{j\mu} - \Delta_\mu \phi_j \tag{25}
$$

associated with the change in the reference point on the unit sphere from $\mathbf{N}_0$ to $\mathbf{N}_0'$, with ϕ_j equal to the area of the spherical triangle formed by $\mathbf{n}_j$, $\mathbf{N}_0$ and $\mathbf{N}_0'$. Finally the area of any triangle on the sphere is uncertain modulo 4π and so the effective action should be invariant under

$$A_{j\mu} \to A_{j\mu} + 4\pi. \tag{26}$$

The simplest local action which is invariant under (25) and (26) is that of *compact U(1) quantum electrodynamics* and so we have

$$Z = \int \prod_{j\mu} dA_{j\mu} \exp\left(\frac{1}{e^2}\sum_{\square}\cos\left(\frac{1}{2}\epsilon_{\mu\nu\lambda}\Delta_\nu A_{j\lambda}\right) - iS\sum_j \eta_j A_{j\tau}\right), \tag{27}$$

for large g; comparison with the large g expansion shows that the coupling $e^2 \sim g^2$. As in Section 3 our analysis is aided by replacing the cosine interaction in (27) by a Villain sum over periodic Gaussians:

$$Z = \sum_{\{q_{\bar{j}\mu}\}} \int \prod_{j\mu} dA_{j\mu} \exp\left(-\frac{1}{2e^2}\sum_{\square}\left(\frac{1}{2}\epsilon_{\mu\nu\lambda}\Delta_\nu A_{j\lambda} - 2\pi q_{\bar{j}\mu}\right)^2 - iS\sum_j \eta_j A_{j\tau}\right), \tag{28}$$

where $q_{\bar{j}\mu}$ are integers on the links of the dual lattice, which pierce the plaquettes of the direct lattice.

We will now perform a series of exact manipulations on (28): our final result, in (35), will be a demonstration of its exact equivalence to another height model, but now with the interface 3=2+1 dimensional. As in Section 3, this interface model is obtained after a duality mapping and has only positive weights. This last fact, of course, makes it much more amenable to a standard statistical analysis. This first step in the duality transformation is to rewrite (28) by the Poisson summation formula:

$$\sum_{\{q_{\bar{j}\mu}\}} \exp\left(-\frac{1}{2e^2}\sum_{\square}\left(\frac{1}{2}\epsilon_{\mu\nu\lambda}\Delta_\nu A_{j\lambda} - 2\pi q_{\bar{j}\mu}\right)^2\right)$$

$$= \sum_{\{a_{\bar{j}\mu}\}} \exp\left(-\frac{e^2}{2}\sum_{\bar{j}} a_{\bar{j}\mu}^2 - i\sum_{\square}\frac{1}{2}\epsilon_{\mu\nu\lambda}a_{\bar{j}\mu}\Delta_\nu A_{j\lambda}\right), \tag{29}$$

where $a_{\bar{j}\mu}$ (like $q_{\bar{j}\mu}$) is an integer-valued vector field on the links of the dual lattice. Next, we write the Berry phase in a form more amenable to duality transformations. Choose a 'background' $a_{\bar{j}\mu} = a_{\bar{j}}^0$ flux which satisfies

$$\epsilon_{\mu\nu\lambda}\Delta_\nu a_{\bar{j}\lambda}^0 = \eta_j \delta_{\mu\tau}, \tag{30}$$
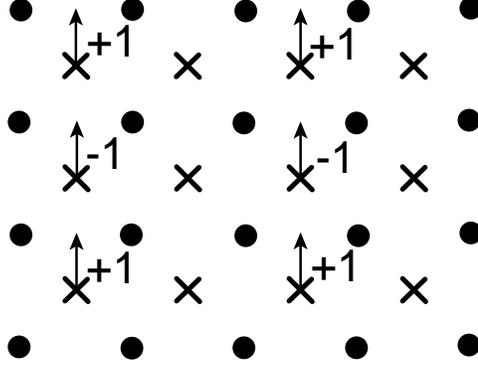
17

Fig. 7. Specification of the non-zero values of the fixed field $a^0_{\bar{j}\mu}$. The circles are the sites of the direct lattice, j, while the crosses are the sites of the dual lattice, $\bar{j}$; the latter are also offset by half a lattice spacing in the direction out of the paper (the $\mu = \tau$ direction). The $a^0_{\bar{j}\mu}$ are all zero for $\mu = \tau, x$, while the only non-zero values of $a^0_{\bar{j}y}$ are shown above. Notice that the a^0 flux obeys (30).

where j is the direct lattice site in the center of the plaquette defined by the curl on the left-hand-side. Any integer-valued solution of (30) is an acceptable choice for $a^0_{\bar{j}\mu}$, and a convenient choice is shown in Fig 7. Using (30) to rewrite the Berry phase in (28), applying (29), and shifting $a_{\bar{j}\mu}$ by the integer $2Sa^0_{\bar{j}\mu}$, we obtain a new exact representation of Z in (28):

$$Z = \sum_{\{a_{\bar{j}\mu}\}} \int \prod_{j\mu} dA_{j\mu} \exp\left(-\frac{e^2}{2}\sum_{\bar{j},\mu}(a_{\bar{j}\mu} - 2Sa^0_{\bar{j}\mu})^2 - i\sum_{\square}\frac{1}{2}\epsilon_{\mu\nu\lambda}a_{\bar{j}\mu}\Delta_\nu A_{j\lambda}\right). (31)$$

The integral over the $A_{j\mu}$ can be performed independently on each link, and its only consequence is the imposition of the constraint $\epsilon_{\mu\nu\lambda}\Delta_\nu a_{\bar{j}\lambda} = 0$. We solve this constraint by writing $a_{\bar{j}\mu}$ as the gradient of a integer-valued height $h_{\bar{j}}$ on the sites of the dual lattice, and so obtain

$$Z = \sum_{\{h_{\bar{j}}\}} \exp\left(-\frac{e^2}{2}\sum_{\bar{j},\mu}(\Delta_\mu h_{\bar{j}} - 2Sa^0_{\bar{j}\mu})^2\right). \tag{32}$$

This is the 2+1 dimensional height model in almost its final form. Before we proceed to an analysis of (32), we pause for a paragraph to make some parenthetic remarks on the application of the above approach to one dimension.

Precisely the same approach as above can be applied to SU(2) symmetric spin chains which we can model by the obvious generalization of (22) to 1+1 dimensions. In the large g limit, we proceed with the same set of duality
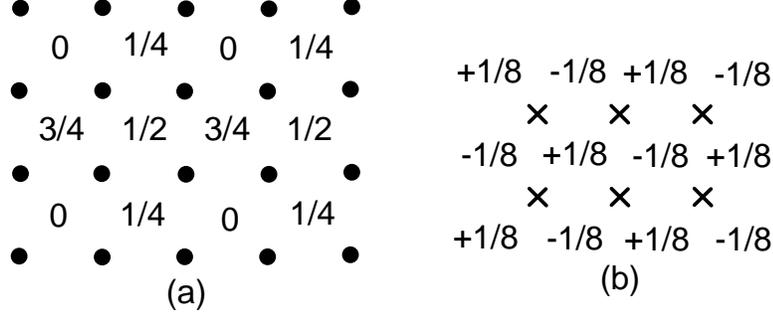
18

Fig. 8. Specification of the non-zero values of the fixed fields (a) $\mathcal{X}_{\bar{j}}$ and (b) $\mathcal{Y}_{j\mu}$ introduced in (34). The notational conventions are as in Fig 7. Only the $\mu = \tau$ components of $\mathcal{Y}_{j\mu}$ are non-zero, and these are shown in (b).

mappings, and in place of (32) we obtain the partition function

$$Z_1 = \sum_{\{a_{\bar{j}}\}} \delta_{\Delta_\mu a_{\bar{j}},0} \exp\left(-\frac{e^2}{2}\sum_{\bar{j}}(a_{\bar{j}} - 2S\ell_{\bar{j}\mu})^2\right). \tag{33}$$

The zero gradient constraint on $a_{\bar{j}}$ (to be contrasted with the zero curl constraint on $a_{\bar{j}\mu}$ in 2+1 dimensions) means that it takes a single fixed value through the entire system. For integer S, the value $a_{\bar{j}} = S$ minimizes the action (its action per site is $e^2 S^2/2$, to be contrasted with the two-fold degenerate BC states with $a_{\bar{j}} = S - 1, S + 1$ with action per site $e^2(S^2 + 1)/2)$, and yields a 'featureless' state with no broken symmetry: this is, of course the Haldane gap state expected for SU(2) symmetric, integer S, spin chains, as discussed in Section 3.1. For half-odd-integer S, there is BC order, as the action in minimized by the two-fold degenerate values $a_{\bar{j}} = S + 1/2, S - 1/2$. All of these results in 1+1 dimensions are in complete accord with the results obtained in Section 3 for large g, and with the known properties of quantum spin chains.

Now we return to the 2+1 dimensional case of interest in this section, and proceed with our interrupted analysis of (32). We can convert the "frustration" $a_{\bar{j}\mu}^0$ in (32) into offsets for the allowed height values (as in Section 3) by decomposing it into curl and divergence free parts and writing it in terms of new fixed fields, $\mathcal{X}_{\bar{j}}$ and $\mathcal{Y}_{j\mu}$ as follows:

$$a_{\bar{j}\mu}^0 = \Delta_\mu \mathcal{X}_{\bar{j}} + \epsilon_{\mu\nu\lambda}\Delta_\nu \mathcal{Y}_{j\lambda}. \tag{34}$$

The values of these new fields are shown in Fig 8. Inserting (34) into (32), we can now write the height model in its simplest form [10–12]

$$Z_h = \sum_{\{H_{\bar{j}}\}} \exp\left(-\frac{e^2}{2}\sum_{\bar{j}}(\Delta_\mu H_{\bar{j}})^2\right), \tag{35}$$

19

where

$$H_{\bar{\jmath}} \equiv h_{\bar{\jmath}} - 2S\mathcal{X}_{\bar{\jmath}} \tag{36}$$

is the new height variable we shall work with. Notice that the $\mathcal{Y}_{j\mu}$ have dropped out, while the $\mathcal{X}_{\bar{\jmath}}$ act only as fractional offsets (for S not an even integer) to the integer heights. From (36) we see that for half-odd-integer S the height is restricted to be an integer on one of the four sublattices, an integer plus $1/4$ on the second, an integer plus $1/2$ on the third, and an integer plus $3/4$ on the fourth; the fractional parts of these heights are as shown in Fig 8a; the steps between neighboring heights are always an integer plus $1/4$, or an integer plus $3/4$. For S an odd integer, the heights are integers on one square sublattice, and half-odd-integers on the second sublattice. Finally for even integer S the offset has no effect and the height is an integer on all sites. We discuss these classes of S values in turn in the following subsections.

(It is worth emphasizing here that the height model Z_h in (35) only offers a description of the large g paramagnetic phase of the model Z in (22) in 2+1 dimensions. The small g Néel ordered state is not one of the phases of Z_h, nor is the critical point describing the onset of magnetic order; an extension of Z_h to include the Néel state was discussed in [8], but will not be presented here. This should be contrasted with the situation in 1+1 dimensions discussed in Section 3; there height models like Z_{XY} in (20) can describe all the phases and critical points of the quantum spin chain, including the TL phase, which is a state with quasi-long-range Néel order).

4.1   S even integer

Unlike the two-dimensional case, three-dimensional height models generically have no roughening transition, and the interface is always smooth. With all heights integers, the smooth phase breaks no symmetries. So like the case of integer S in quantum spin chains (Section 3.1), square lattice antiferromagnets with S even integer can have a paramagnetic ground state with a spin gap and no broken symmetries. This is in accord with the exact ground state for a $S = 2$ antiferromagnet on the square lattice found by Affleck et $al.$ [14], the AKLT state. The structure of this state is identical to that of the paramagnetic state of the φ^4 field theory in 2+1 dimensions (Eqn (9) with $c_x = c_y$), with a stable $S = 1$ spin exciton excitation. So the critical point between the magnetic Néel state and the spin gap state should also be described by the φ^4 field theory. As we noted above, this critical point is not contained within Z_h.
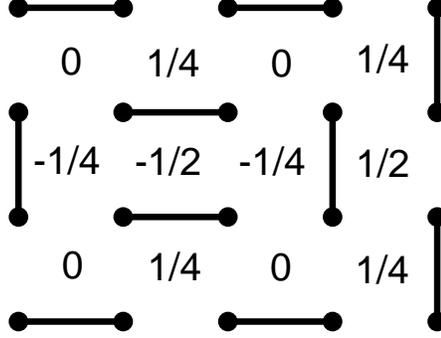
Fig. 9. Mapping between the quantum dimer model and the interface model Z in (35). Each dimer on the direct lattice is associated with a step in height of $\pm 3/4$ on the link of the dual lattice that crosses it. All other height steps are $\pm 1/4$. Each dimer represents a singlet valence between the sites, as in Fig 2.

4.2   S half-odd-integer

Now the heights of the interface model can take four possible values, which are integers plus the offsets on the four square sublattices shown in Fig 8a. As in Section 4.1, the interface is always smooth, but as in Section 3.2, any smooth interface must break a lattice symmetry with the development of bond-centered charge (BC) order and this allows a number of distinct spin gap ground states of the lattice antiferromagnet. Consistent with these theoretical predictions, numerical studies of the frustrated spin model (23) have produced evidence for BC order in the state contiguous to the Néel state: see [15,16] for recent results.

It is useful, first, to obtain a simple physical interpretation of the interface model in the language of the $S = 1/2$ antiferromagnet [13]. From Fig 8a it is clear that nearest neighbor heights can differ either by $1/4$ or $3/4$ (modulo integers). To minimize the action in (35), we should choose the interface with the largest possible number of steps of $\pm 1/4$. However, the interface is frustrated, and it is not possible to make all steps $\pm 1/4$ and at least a quarter of the steps must be $\pm 3/4$. Indeed, there is a precise one-to-one mapping between interfaces with the minimal number of $\pm 3/4$ steps (we regard interfaces differing by a uniform integer shift in all heights as equivalent) and the dimer coverings of the square lattice: the proof of this claim is illustrated in Fig 9. We identify each dimer with a singlet valence bond between the spins (the ellipses in Fig 2), and so each interface corresponds to a quantum state with each spin locked in the a singlet valence bond with a particular nearest neighbor. Fluctuations of the interface in imaginary time between such configurations correspond to quantum tunneling events between such dimer states, and an effective Hamiltonian for this is provided by the quantum dimer model [17,18].

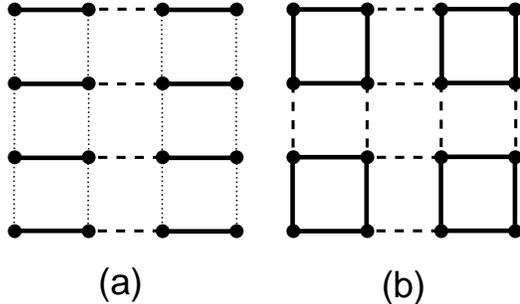The nature of the possible smooth phases of the interface model are easy

Fig. 10. Sketch of the two simplest possible states with bond-centered charge (BC) order for $S = 1/2$ on the square lattice: (a) the columnar spin-Peierls states, and (b) plaquette state. The different values of the $\langle \mathbf{S}_i \cdot \mathbf{S}_j \rangle$ on the links are encoded by the different line styles. Both states are 4-fold degenerate; an 8-fold degenerate state, with superposition of the above orders, also appears as a possible ground state of the generalized interface model.

to determine from the above picture, and by standard techniques from statistical theory which have been reviewed elsewhere [11,8,13,19]. Interfaces with average height $\langle H_{\bar{j}} \rangle = 1/8, 3/8, 5/8, 7/8$ (modulo integers) correspond to the four-fold degenerate BC ordered states in Fig 10a, while those with $\langle H_{\bar{j}} \rangle = 0, 1/4, 1/2, 3/4$ (modulo integers) correspond to the four-fold degenerate plaquette BC states in Fig 10b. All other values of $\langle H_{\bar{j}} \rangle$ are associated with eight-fold degenerate BC states with a superposition of the orders in Fig 10a and b.

It is interesting to note here that the symmetry of the state in Fig 10a is identical to the symmetry of the coupled ladder Hamiltonian illustrated in Fig 1: so the system has spontaneously decided to arrange itself in the form of a coupled ladder. Whether the BC ordering is spontaneous (as it is here) or explicitly present in the Hamiltonian (as in Section 2), the nature of the non-zero spin excitations should be the same. So the confinement argument of Fig 3b applies here too, and there are no free $S = 1/2$ spinons in the BC state. The elementary excitation is a $S = 1$ spin exciton. This should be contrasted with the $S = 1/2$ quantum spin chain in Section 3.2, where the BC state had spinon excitations.

We are now finally in a position to explain a central step in the analysis of Section 2: the neglect of Berry phases in the theory of the magnetic critical point for the coupled ladder antiferromagnet. We have seen here that the primary effect of the Berry phases is to induce BC order in the spin gap state. However, such "order" is already present explicitly in the Hamiltonian of the coupled ladder antiferromagnet, which has two sites per unit cell: the Hamiltonian picks out one of the four BC states and "dimer" fluctuations to the other BC states are suppressed. So we need only focus on the fluctuations of the magnetic order, and these are captured by the φ^4 field theory.

The nature of the crossover between the Néel and BC states for $S = 1/2$ quantum spin models with the full square lattice symmetry (like H in (23)) is far more subtle, and was recently discussed at some length in Ref [8]. Here, both the Néel and BC orders can become critical, and so we cannot naively assert the irrelevance of the Berry phases. One appealing scenario [15,8], supported by recent numerical studies [15], is that the crossover occurs via two transitions: with increasing g, there is first a transition at $g = g_{c1}$ to a state with co-existing Néel and BC order (only the BC fluctuations are critical at g_{c1} are these are described by a Z_4 clock model), and then a transition at $g = g_{c2} > g_{c1}$ where Néel order disappears. The second transition at g_{c2} is just as in the coupled ladder antiferromagnet, and is therefore described by the φ^4 field theory: there is well-formed BC order on the either side of $g = g_{c2}$, and it is immaterial here whether this order was explicitly present in the Hamiltonian or spontaneously induced. Indeed, this was secretly the reason we chose to consider the coupled ladder antiferromagnet in our early discussion.

4.3 S odd integer

This case is similar to that S half-odd-integer, and we will not consider it in detail. The Berry phases again induce BC order in the spin gap state, but this order need only lead to a two-fold degeneracy.

5 Magnetic transitions in d-wave superconductors

We have so far considered a variety of magnetic transitions in correlated "Mott" insulators, which have an electron density commensurate with the number of available orbitals. Cuprate high temperature superconductivity appears when such a Mott insulator on the square lattice is doped by a finite density of mobile carriers. All of the available experimental evidence supports the proposal that, apart from some inhomogeneous charge ordered insulating states, the ground state of the doped Mott insulator is a superconductor. In particular, there is no clear-cut evidence for a metallic Fermi liquid state up to a moderate density of holes. Consequently, we will focus our attention on the superconducting ground state in the remainder of this paper. This is to be contrasted with the approach of [20] which examines transitions in metallic states at non-zero temperature.

It is now natural to study the interplay of the Néel magnetic order found in the insulator and the superconducting order of the doped system. (The charge order discussed in Section 4 also plays an important role in the superconductor, but we will not focus attention on this aspect here — see [21] for a recent

review.) The experimental evidence indicates that this crossover proceeds via an intermediate state with *co-existence* of magnetic and superconducting order. Furthermore, the magnetic order is no longer in the simple two-sublattice Néel configuration, but oscillates at a wavevector $K \neq (\pi, \pi)$. So instead of expressing the electron spin as $S_{j\alpha} = \eta_j \varphi_\alpha(r_j)$, which is implied by (7) and the subsequent coarse-graining of $\mathbf{n}$ to φ_α, we now write

$$S_{j\alpha} = \Phi_\alpha(r_j)e^{iKr} + \text{c.c.}, \tag{37}$$

where $\Phi_\alpha(r, \tau)$ a 3-component, *complex* quantum field; Φ_α is required to be complex as along as the magnetic state does not have a two sublattice structure, which is only the case for ordering wavevectors (π, π) and $(0, \pi)$. Also, the experimental evidence also indicates that the magnetic order is *collinear*, and not spiral; this is the case if $\epsilon_{\alpha\beta\gamma}\langle\Phi_\beta\rangle\langle\Phi_\gamma^*\rangle = 0$.

With this reasoning, we are led to consider the quantum transition between a superconducting state with co-existing magnetic spin-density-wave order at wavevector K ($\langle\Phi_\alpha\rangle \neq 0$ in the SC+SDW state) to an ordinary superconductor ($\langle\Phi_\alpha\rangle = 0$ in the SC state). Clearly, the field Φ_α should be a degree of freedom in any theory for this transition. However, in a superconductor there are additional fermionic excitations which carry spin $S = 1/2$, the Bogoliubov quasiparticles, and we have to examine their influence on the critical properties. This is especially the case in a d-wave superconductor, in which the energy of the quasiparticles vanishes at four 'nodal' points in the Brillouin zone.

To address this issue, let us review the standard BCS mean-field theory for a d-wave superconductor on the square lattice. We consider the Hamiltonian

$$H_{tJ} = \sum_k \varepsilon_k c_{k\sigma}^\dagger c_{k\sigma} + J_1 \sum_{\langle ij \rangle} \mathbf{S}_i \cdot \mathbf{S}_j \tag{38}$$

where $c_{j\sigma}$ is the annihilation operator for an electron on site j with spin $\sigma = \uparrow, \downarrow$, $c_{k\sigma}$ is its Fourier transform to momentum space, ε_k is the dispersion of the electrons (it is conventional to choose $\varepsilon_k = -2t_1(\cos(k_x) + \cos(k_y)) - 2t_2(\cos(k_x + k_y) + \cos(k_x - k_y)) - \mu$, with $t_{1,2}$ the first/second neighbor hopping and μ the chemical potential), and the J_1 term is the same as that in (23) with

$$S_{j\alpha} = \frac{1}{2}c_{j\sigma}^\dagger \sigma_{\sigma\sigma'}^\alpha c_{j\sigma'} \tag{39}$$

and σ^α the Pauli matrices. We will consider the consequences of the J_2 term in (23) for the superconductor in Section 6 below. Applying the BCS mean-field

decoupling to H_{tJ} we obtain the Bogoliubov Hamiltonian

$$H_{BCS} = \sum_k \varepsilon_k c_{k\sigma}^\dagger c_{k\sigma} - \frac{J_1}{2} \sum_{j\mu} \Delta_\mu \left(c_{j\uparrow}^\dagger c_{j+\hat{\mu},\downarrow}^\dagger - c_{j\downarrow}^\dagger c_{j+\hat{\mu},\uparrow}^\dagger \right) + \text{h.c.}. \tag{40}$$

For a wide range of parameters, the ground state energy optimized by a $d_{x^2-y^2}$ wavefunction for the cooper pairs: this corresponds to the choice $\Delta_x = -\Delta_y = \Delta_{x^2-y^2}$. The value of $\Delta_{x^2-y^2}$ is determined by minimizing the energy of the BCS state

$$E_{BCS} = J_1 |\Delta_{x^2-y^2}|^2 - \int \frac{d^2k}{4\pi^2} \left[E_k - \varepsilon_k \right] \tag{41}$$

where the fermionic quasiparticle dispersion is

$$E_k = \left[\varepsilon_k^2 + |J_1 \Delta_{x^2-y^2}(\cos k_x - \cos k_y)|^2 \right]^{1/2}. \tag{42}$$

The energy of the quasiparticles, E_k, vanishes at the four points $(\pm Q, \pm Q)$ at which $\varepsilon_k = 0$. We are especially interested in the low energy quasiparticles in the vicinity of these points, and so we perform a gradient expansion of H_{BCS} near each of them. We label the points $Q_1 = (Q, Q)$, $Q_2 = (-Q, Q)$, $Q_3 = (-Q, -Q)$, $Q_4 = (Q, -Q)$ and write

$$c_{j\sigma} = f_{1\sigma}(x_j)e^{iQ_1 x_j} + f_{2\sigma}(x_j)e^{iQ_2 x_j} + f_{3\sigma}(x_j)e^{iQ_3 x_j} + f_{4\sigma}(x_j)e^{iQ_4 x_j}, \tag{43}$$

while assuming the $f_{1-4,\sigma}(x)$ are slowly varying functions of x. We also introduce the bispinors $\Psi_1 = (f_{1\uparrow}, f_{3\downarrow}^\dagger, f_{1\downarrow}, -f_{3\uparrow}^\dagger)$, and $\Psi_2 = (f_{2\uparrow}, f_{4\downarrow}^\dagger, f_{2\downarrow}, -f_{4\uparrow}^\dagger)$, and then express H_{BCS} in terms of $\Psi_{1,2}$ while performing a spatial gradient expansion. This yields the following effective action for the fermionic quasiparticles:

$$\mathcal{S}_\Psi = \int d\tau d^2x \left[\Psi_1^\dagger \left(\partial_\tau - iv_F \tau^z \partial_x - iv_\Delta \tau^x \partial_y \right) \Psi_1 \right.$$
$$\left. + \Psi_2^\dagger \left(\partial_\tau - iv_F \tau^z \partial_y - iv_\Delta \tau^x \partial_x \right) \Psi_2 \right], \tag{44}$$

where we have rotated our spatial co-ordinate system by $45°$, and the $\tau^{x,z}$ are 4×4 matrices which are block diagonal, the blocks consisting of 2×2 Pauli matrices. The velocities $v_{F,\Delta}$ are given by the conical structure of E_k near the Q_{1-4}: we have $v_F = |\nabla_k \varepsilon_k|_{k=Q_a}|$ and $v_\Delta = |J_1 \Delta_{x^2-y^2} \sqrt{2} \sin(Q)|$.

We are now in a position to discuss the quantum field theory of the transition from the SC+SDW to the SC state in term of the Φ_α and $\Psi_{1,2}$ degrees of freedom. First, we can write down an action for Φ_α along the lines of that for φ_α in the insulator: this will have a structure very similar to that of (9)

25

(the complex nature of Φ_α induces additional quartic terms which we will not discuss here—the reader is referred to another review by the author [21] for details on this point). The action will also contain the terms in $\mathcal{S}_\Psi$ in (44), and it remains to discuss terms which may couple the Φ_α and $\Psi_{1,2}$. The simplest possible terms are cubic interaction terms like $\Phi_\alpha \Psi_1 \Psi_1$ etc. However by comparing the momentum dependencies in (37) and (43) with (39) it is easy to see that such terms will survive after averaging over space only if the special commensurability conditions $K = (2Q, 2Q)$, or $K = (2Q, 0)$, are satisfied. In general this will not be the case, and experimental evidence also does not support this possibility. Therefore, we will assume in the remainder of this section that these commensurability conditions are not satisfied: the theory for the case $K = (2Q, 2Q)$, $Q = \pi/2$ was considered in Ref. [22], and has some formal similarities to the theory to be considered in Section 6 in a different physical context.

In the absence of special commensurability conditions, the simplest term which can couple the Φ_α and $\Psi_{1,2}$ is

$$\kappa \int d^2r d\tau |\Phi_\alpha|^2 \left(\Psi_1^\dagger \Psi_1 + \Psi_2^\dagger \Psi_2 \right). \tag{45}$$

However a simple scaling argument shows that the coupling κ is irrelevant at the SC+SDW to SC critical point. To see this, imagine that the critical point is described by the $\kappa = 0$ point, where the Φ_α and $\Psi_{1,2}$ fields are decoupled. This point is actually a fixed point of the renormalization group and is invariant under scaling transformations. From (44) we see that the scaling dimensions of $\Psi_{1,2}$ is 1, while that of $|\Phi_\alpha|^2$ is $(3 - 1/\nu)$, where ν is the correlation length exponent. So from (45) we conclude that the scaling dimension of κ is $(1/\nu - 2)$. The exponent ν is determined by a theory like that in (9) for Ψ_α and all such theories have $\nu > 1/2$, the mean-field exponent. Consequently the scaling dimension of κ is negative, and the decoupled $\kappa = 0$ fixed point describes the SC+SDW to SC quantum phase transition. The critical magnetic fluctuations are associated with Φ_α, and the fermionic, $S = 1/2$ quasiparticles $\Psi_{1,2}$ are merely innocent spectators.

This last result is quite powerful, as it implies that we can apply the results of the quantum transition in the insulator, discussed in Section 2, essentially unchanged to the magnetic fluctuations in the cuprate high temperature superconductors. Such a proposal was first made in Ref. [23,24], and leads to the prediction that the $S = 1$ exciton should survive as a stable excitation in the SC state near its transition to the SC+SDW state, and that this should be evident as a sharp "resonance" in dynamic neutron scattering: such a resonance appears to have been observed in a number of experiments [25–29]. The framework of the SC+SDW to SC transition has also been used to understand dynamic spin correlations in the presence of Zn impurities [30,31], and

to explore the phase diagram in the presence of an applied magnetic field [32]: the results have been quantitatively compared with neutron scattering experiments [33–36].

6   Transition between BCS superconductors

In this final section, we will consider one of the simplest examples of a non-trivial quantum critical point in two spatial dimensions which, surprisingly, was only discovered recently [38,39]. The two phases on either side of the critical point are described by an entirely conventional BCS theory: they differ only in the symmetry of the Cooper pair wavefunction, dependent upon the relative co-ordinates of the paired electrons. At $T = 0$, BCS theory provides an accurate description of the low energy properties everywhere except at the point which separates the two phases: this is probably the only known example of the failure of BCS theory in two (or higher) dimensions in a superconducting ground state. At $T > 0$, this failure broadens into the "quantum critical" region which should be easily experimentally detectable: we will not discuss these $T > 0$ issues here, and instead refer the reader to other reviews [1].

Our original motivation for examining transitions between BCS superconductors was provided by photoemission experiments [37] which observed an anomalous broadening of the quasiparticle spectrum. We will discuss this further in Section 6.3, but will motivate the problem now on theoretical grounds. The Hubbard model on a square lattice is believed to provide a good starting point for studying the physics of the cuprate superconductors. There is now good evidence that for electron densities close to half-filling, the primary instability of the Fermi liquid state is to a BCS superconductor with $d_{x^2-y^2}$ symmetry [40], whose mean-field theory was presented in Section 5. The opposite limit of a low density of electrons, well away from half-filling, has also been examined theoretically [41,42], and the low density expansion permits reliable predictions to be made: it was found that the ground state was again a BCS superconductor, but now the pairs had a distinct d_{xy} symmetry (in the presence of a square lattice, the $d_{x^2-y^2}$ and d_{xy} states are not degenerate, as they would be in free space). Here we will answer the simple question: how does the ground state evolve from between these limits with qualitatively different wavefunctions ?

Rather than working the full complexities of the Hubbard model, we follow the strategy of Section 5 and work with the simplest phenomenological model that contains the two phases we are interested in. We want to extend H_{tJ} in (38) so that a BCS mean-field theory will permit a region with d_{xy} superconductivity. Clearly this will be possible if we have a pairing interaction along the $(1, \pm 1)$ directions of the square lattice; so we extend H_{tJ} to allow for a second-neighbor
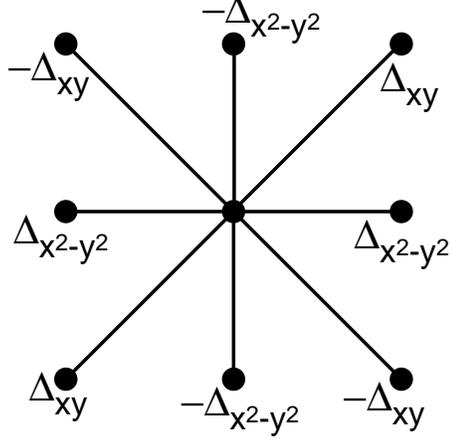
Fig. 11. Values of the pairing amplitudes, $-\langle c_{i\uparrow}c_{j\downarrow} - c_{i\downarrow}c_{j\uparrow}\rangle$ with i the central site, and j is one of its 8 near neighbors.

exchange along the diagonals, J_2, as in (23):

$$\widetilde{H}_{tJ} = \sum_k \varepsilon_k c_{k\sigma}^\dagger c_{k\sigma} + J_1 \sum_{\langle ij \rangle} \mathbf{S}_i \cdot \mathbf{S}_j + J_2 \sum_{\text{nnn } ij} \mathbf{S}_i \cdot \mathbf{S}_j. \tag{46}$$

We will follow the evolution of the ground state of $\widetilde{H}_{tJ}$ as a function of J_2/J_1. We expect that the universal properties of this route will be similar to that of the Hubbard model as a function of carrier concentration, in light of the studies of the latter model quoted above.

6.1 BCS Theory

We begin with a standard BCS analysis of $\widetilde{H}_{tJ}$ which closely parallels that presented in Section 5. The mean-field Hamiltonian is now modified from (40) to

$$\widetilde{H}_{BCS} = \sum_k \varepsilon_k c_{k\sigma}^\dagger c_{k\sigma} - \frac{J_1}{2} \sum_{j,\mu} \Delta_\mu (c_{j\uparrow}^\dagger c_{j+\hat{\mu},\downarrow}^\dagger - c_{j\downarrow}^\dagger c_{j+\hat{\mu},\uparrow}^\dagger) + \text{h.c.}$$
$$- \frac{J_2}{2} {\sum_{j,\nu}}' \Delta_\nu (c_{j\uparrow}^\dagger c_{j+\hat{\nu},\downarrow}^\dagger - c_{j\downarrow}^\dagger c_{j+\hat{\nu},\uparrow}^\dagger) + \text{h.c.}, \tag{47}$$

where the second summation over ν is along the diagonal neighbors $\hat{x} + \hat{y}$ and $-\hat{x} + \hat{y}$. To obtain d_{xy} pairing along the diagonals, we choose $\Delta_{x+y} = -\Delta_{-x+y} = \Delta_{xy}$. We summarize our choices for the spatial structure of the pairing amplitudes (which determine the Cooper pair wavefunction) in Fig 11. The values of $\Delta_{x^2-y^2}$ and Δ_{xy} are to be determined by minimizing the ground
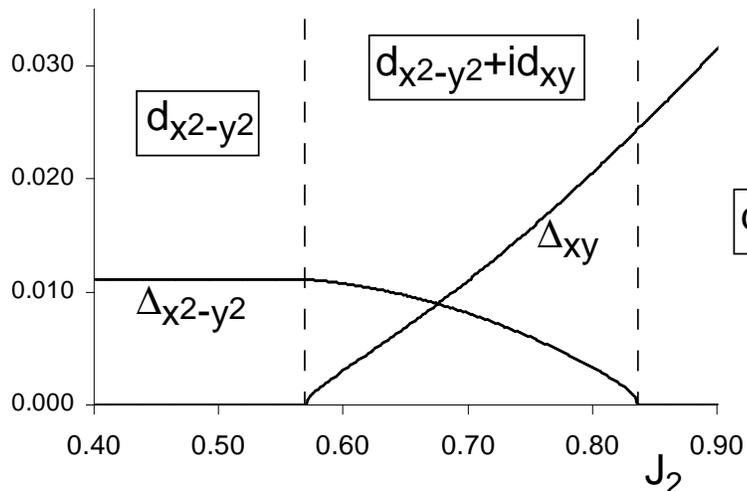
Fig. 12. BCS solution of the phenomenological Hamiltonian $\widetilde{H}_{tJ}$ in (46). Shown are the optimum values of the pairing amplitudes $|\Delta_{x^2-y^2}|$ and $|\Delta_{xy}|$ as a function of J_2 for $t_1 = 1$, $t_2 = -0.25$, $\mu = -1.25$, and J_1 fixed at $J_1 = 0.4$. The relative phase of the pairing amplitudes was always found to obey (50). The dashed lines denote locations of phase transitions between $d_{x^2-y^2}$, $d_{x^2-y^2} + id_{xy}$, and d_{xy} superconductors. The pairing amplitudes vanish linearly at the two critical points, corresponding to the exponent $\beta_{BCS} = 1$ in (53); the slight rounding at the end points apparent in the figure is a consequence of the finite step-size used in numerical evaluation of the integral in (48). Combining these results with those of [40–42] we conclude that the more realistic Hubbard model will show the same sequence of phases as those above as a function of increasing doping.

state energy (generalizing (41))

$$E_{BCS} = J_1|\Delta_{x^2-y^2}|^2 + J_2|\Delta_{xy}|^2 - \int \frac{d^2k}{4\pi^2} \left[E_k - \varepsilon_k\right] \tag{48}$$

where the quasiparticle dispersion is now (generalizing (42))

$$E_k = \left[\varepsilon_k^2 + |J_1\Delta_{x^2-y^2}(\cos k_x - \cos k_y) + 2J_2\Delta_{xy}\sin k_x \sin k_y|^2\right]^{1/2}. \tag{49}$$

Notice that the energy depends upon the relative phase of $\Delta_{x^2-y^2}$ and Δ_{xy}: this phase is therefore an observable property of the ground state.

It is a simple matter to numerically carry out the minimization of (49), and the results for a typical choice of parameters are shown in Fig 12 as a function J_2/J_1. One of the two amplitudes $\Delta_{x^2-y^2}$ or Δ_{xy} is always non-zero and so the ground state is always superconducting. The transition from pure $d_{x^2-y^2}$ superconductivity to pure d_{xy} superconductivity occurs via an intermediate phase in which *both* order parameters are non-zero. Furthermore, in this regime, their

29

relative phase is found to be pinned to $\pm\pi/2$ *i.e.*

$$\arg(\Delta_{xy}) = \arg(\Delta_{x^2-y^2}) \pm \pi/2 \tag{50}$$

The reason for this pinning can be intuitively seen from (49): only for these values of the relative phase does the equation $E_k = 0$ never have a solution. In other words, the gapless nodal quasiparticles of the $d_{x^2-y^2}$ superconductor (and also those of the d_{xy} superconductor) acquire a finite energy gap when a secondary pairing with relative phase $\pm\pi/2$ develops. By a level repulsion picture, we can expect that gapping out the low energy excitations should help lower the energy of the ground state. The intermediate phase obeying (50) is called a $d_{x^2-y^2} + id_{xy}$ superconductor.

The choice of the sign in (50) leads to an overall two-fold degeneracy in the choice of the wavefunction for the $d_{x^2-y^2} + id_{xy}$ superconductor. This choice is related to the breaking of time-reversal symmetry, and implies that the $d_{x^2-y^2} + id_{xy}$ phase is characterized by the non-zero expectation value of a Z_2 Ising order parameter; the expectation value of this order vanishes in the two phases (the $d_{x^2-y^2}$ and d_{xy} superconductors) on either side of the $d_{x^2-y^2} + id_{xy}$ superconductor. As is conventional, we will represent the Ising order by a real scalar field ϕ. Fluctuations of ϕ become critical near both of the phase boundaries in Fig 12. As we will explain in Section 6.2 below, the critical theory for ϕ fluctuations is *not* the usual ϕ^4 field theory which describes the ordinary Ising transition in three spacetime dimensions.

Near the phase boundary from $d_{x^2-y^2}$ to $d_{x^2-y^2} + id_{xy}$ superconductivity it is clear that we can identify

$$\phi = i\Delta_{xy}, \tag{51}$$

(in the gauge where $\Delta_{x^2-y^2}$ is real). We can now expand E_{BCS} in (48) for small ϕ (with $\Delta_{x^2-y^2}$ finite) and find a series with the structure [43,44]

$$E_{BCS} = E_0 + s\phi^2 + v|\phi|^3 + \ldots, \tag{52}$$

where s, v are coefficients and the ellipses represent regular higher order terms in even powers of ϕ; s can have either sign, whereas v is always positive. Notice the non-analytic $|\phi|^3$ term that appears in the BCS theory — this arises from an infrared singularity in the integral in (48) over E_k at the four nodal points of the $d_{x^2-y^2}$ superconductor, and is a preliminary indication that the transition differs from that in the ordinary Ising model. We will achieve a deeper understanding of this non-analyticity when we consider fluctuations in Section 6.2. We can optimize ϕ by minimizing E_{BCS} in (52)— this shows

SC+SDW | SC | SC
anisotropic $d_{x^2-y^2}$ superconductivity | $d_{x^2-y^2}$ superconductivity | $d_{x^2-y^2}+id_{xy}$ superconductivity
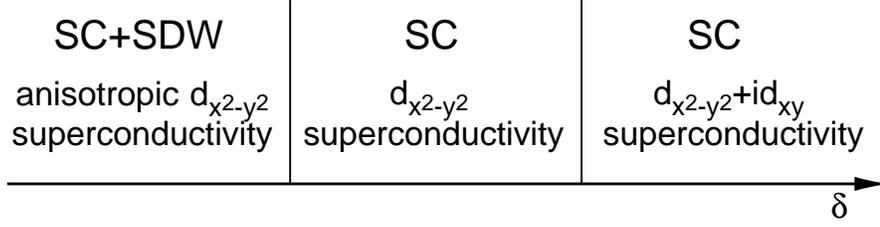
δ

Fig. 13. Conjectured $T = 0$ phase diagram for the cuprate superconductors as a function of increasing hole concentration δ. The theory for the SC+SDW to SDW transition appears in Section 5, while that of the transition describing the onset of $d_{x^2-y^2} + id_{xy}$ order appears in Section 6.2. The second transition may not be on the physical axis for a given cuprate superconductor, but may be nearby in a generalized parameter space.

that $\langle \phi \rangle = 0$ for $s > 0$, and $\langle \phi \rangle \neq 0$ for $s < 0$. So $s \sim (J_2/J_1)_c - J_2/J_1$ where $(J_2/J_1)_c$ is the first critical value in Fig 12. Near this critical point, we find

$$\langle \phi \rangle \sim (s_c - s)^\beta, \tag{53}$$

where we have allowed for the fact that fluctuation corrections will shift the critical point from $s = 0$ to $s = s_c$. The present BCS theory yields the exponent $\beta_{BCS} = 1$; this differs from the usual mean-field exponent $\beta_{MF} = 1/2$, and this is of course due to the non-analytic $|\phi|^3$ term in (52).

An essentially identical structure appears at the second critical point in Fig 12 at the boundary between the $d_{x^2-y^2} + id_{xy}$ and d_{xy} superconductors. The $d_{x^2-y^2}$ and d_{xy} pairing amplitudes exchange roles, and the Ising order parameter for the transition is $\phi = i\Delta_{x^2-y^2}$ (replacing (51)). We will therefore not discuss this case further.

We close this subsection by presenting a unified overview of the quantum phase transitions in the cuprate superconductors we have introduced so far: this is presented in Fig 13. At low, but finite, doping we have the SC+SDW phase which was discussed in Section 5. Here the presence of the SDW order induces spatial anisotropy between the x and y axis (in real space), and so the superconductivity is not purely d-wave, although gapless nodal fermions may be present [45,46]. With increasing δ we have a transition to a SC phase, where the superconducting order is $d_{x^2-y^2}$, and is described by a vanilla BCS theory: this transition was also discussed in Section 5. Finally, the results of [41,42] show that the d_{xy} superconductivity at very low electron density: we have used a phenomenological model of this crossover in the present section to argue that this implies that the next phase with increasing doping should be a $d_{x^2-y^2} + id_{xy}$ superconductor. The full critical theory of this transition appears in the following subsection. In placing the $d_{x^2-y^2} + id_{xy}$ at large doping, we are also following the experimental results of Dagan and Deutscher [47] which we will discuss further in Section 6.3.

We will now present a full theory for the quantum transition between the $d_{x^2-y^2}$ and $d_{x^2-y^2} + id_{xy}$ superconductors: this will allow us to compute the corrections to the predictions of the BCS theory implied by (52).

We have laid much of the ground work for the required field theory in Section 5. In addition to the order parameter ϕ, the field theory should also involve the low energy nodal fermions of the $d_{x^2-y^2}$ superconductor, as described by $\mathcal{S}_\Psi$ in (44). For the ϕ fluctuations, we write down the usual terms permitted near a phase transition with Ising symmetry, and similar to those in (9):

$$\mathcal{S}_\phi = \int d^2r d\tau \left[\frac{1}{2} \left((\partial_\tau \phi)^2 + c^2 (\partial_x \phi)^2 + c^2 (\partial_y \phi)^2 + s\phi^2 \right) + \frac{u}{24}\phi^4 \right]. \qquad (54)$$

Note that, unlike (52), we do not have any non-analytic $|\phi|^3$ terms in the action: this is because we have not integrated out the low energy nodal fermions, and the terms in (54) are viewed as arising from high energy fermions away from the nodal points. Finally, we need to couple the ϕ and $\Psi_{1,2}$ excitations. Their coupling is already contained in the last term in (47): expressing this in terms of the $\Psi_{1,2}$ fermions using (43) we obtain

$$\mathcal{S}_{\Psi\phi} = \int d^2r d\tau \left[\lambda\phi \left(\Psi_1^\dagger \tau^y \Psi_1 - \Psi_2^\dagger \tau^y \Psi_2 \right) \right], \qquad (55)$$

where λ is a coupling constant. The partition function of the full theory is now

$$Z_{did} = \int \mathcal{D}\phi \mathcal{D}\Psi_1 \mathcal{D}\Psi_2 \exp\left(-\mathcal{S}_\Psi - \mathcal{S}_\phi - \mathcal{S}_{\Psi\phi} \right), \qquad (56)$$

where $\mathcal{S}_\Psi$ was in (44). It can now be checked that if we integrate out the $\Psi_{1,2}$ fermions for a spacetime independent ϕ, we do indeed obtain a $|\phi|^3$ term in the effective potential for ϕ.

We begin our analysis of Z_{did} in (56) by following the procedure discussed below (45). Assume that the transition is described by a fixed point with $\lambda = 0$: then as in Section 5, the theory for the transition would be the ordinary ϕ^4 field theory $\mathcal{S}_\phi$, and the nodal fermions would again be innocent spectators (we already know from the presence of the $|\phi|^3$ term in (52) that this assumption cannot be correct, but we wish to see how it is invalidated in a renormalization group analysis). The scaling dimension of ϕ at such a fixed point is $(1 + \eta_I)/2$ (where η_I is the anomalous order parameter exponent at the critical point of the ordinary three dimensional Ising model), while that of $\Psi_{1,2}$ is 1 (as before). Consequently scaling dimension of λ is $(1 - \eta_I)/2 > 0$ (using the known, very

small value of η_I). This positive scaling dimension implies that λ is relevant and the $\lambda = 0$ fixed point is unstable.

Determining the correct critical behavior now requires a full renormalization group analysis of Z_{did}. This has been described in some detail in [48], and we will not reproduce the details here. The main result we need for our purposes is that couplings λ, u, v_F/c and v_Δ/c all reach *non-zero* fixed point values which define a critical point in a new universality class. These fixed point values, and the corresponding critical exponents, can be determined in expansions in either $(3-d)$ [38,39] (where d is the spatial dimensionality) or $1/N$ [49] (where N is the number of fermion species). Indeed the fixed point has the structure of the so-called Higgs-Yukawa model which has been studied extensively in the particle physics literature [50] in a different physical context: quantum Monte Carlo simulation of this model also exist [51], and provide probably the most accurate estimate of the exponents.

The implications of the existence of this finite-coupling critical point are similar to those for (9) in (13). The fermion correlation function $G_1 = \langle \Psi_1 \Psi_1^\dagger \rangle$ obeys

$$G_1(k, \omega) = \frac{\omega + v_F k_x \tau^z + v_\Delta \tau^x}{(v_F^2 k_x^2 + v_\Delta^2 k_y^2 - \omega^2)^{(1-\eta_f)/2}} \tag{57}$$

at low frequencies for $s \geq s_c$. Away from the critical point in the $d_{x^2-y^2}$ superconductor with $s > s_c$, (57) holds with $\eta_f = 0$, and this is the BCS result, with sharp quasi-particle poles in the Green's function. At the critical point $s = s_c$ (57) holds with the fixed point values for the velocities (which satisfy $v_F = v_\Delta = c$) and with the anomalous dimension $\eta_f \neq 0$ — the $(3-d)$ expansion [38] estimate is $\eta_f \approx (3-d)/14$, and the $1/N$ expansion estimate [49] is $\eta_f \approx 1/(3\pi^2 N)$, with $N = 2$. This is clearly non-BCS behavior, and the fermionic quasiparticle pole in the spectral function has been replaced by a branch-cut representing the continuum of critical excitations. The corrections to BCS extend also to correlations of the Ising order ϕ: its expectation value vanishes as (53) with the Monte Carlo estimate $\beta \approx 0.877$ [51]. The critical point correlators of ϕ also obey (13) with the exponent $\eta \approx 0.754$ [51], which is clearly different from the very small value of the exponent η_I at the unstable $\lambda = 0$ fixed point. The value of β is related to η by the usual scaling law $\beta = (1 + \eta)\nu/2$, with $\nu \approx 1.00$ the correlation length exponent (which also differs from the exponent ν_I of the Ising model).

We noted at the beginning of this section that our original motivation for studying the $d_{x^2-y^2}$ to $d_{x^2-y^2} + id_{xy}$ transition was provided by photoemission experiments of Valla *et al.* [37]. In particular these experiments found that the typical quasiparticle energy width was of order $k_B T$. As we have reviewed elsewhere [1], this is a characteristic property of the $T > 0$ quantum critical region of a $T = 0$ critical point which obeys strong hyperscaling properties. In particular, it is essential that the critical point be described by an interacting field theory, with the interaction strengths determined by a finite-coupling fixed point of the renormalization group. This condition is clearly satisfied by Z_{did}: the breakdown of BCS theory at $s = s_c$, which leads to (57) with $\eta_f \neq 0$ at $T = 0$, is directly responsible for quasiparticle lifetimes of order $\hbar/k_B T$ over a finite range of g values in the $T > 0$ quantum critical region. In Ref. [38] it was also shown that the fixed point of Z_{did} was also essentially unique in satisfying such requirements: the only other zero momentum order parameter which led to suitable critical point was that between a $d_{x^2-y^2}$ and a $d_{x^2-y^2} + is$ superconductor.

A more direct probe of the $d_{x^2-y^2} + id_{xy}$ order has been provided by very interesting tunneling measurements of Dagan and Deutscher [47]. They examined the splitting of a zero-bias conductance peak as a function of doping δ and an applied magnetic field, H, perpendicular to the two-dimensional electron gas. They found that this splitting closely tracked the value $\langle \phi \rangle$ as determined by minimizing the energy in (52) extended with a linear coupling to the magnetic field

$$E_{BCS} = E_0 + s\phi^2 + v|\phi|^3 - H\phi. \tag{58}$$

The linear coupling is also just that expected from the fact that the $d_{x^2-y^2} + id_{xy}$ superconductor has a spontaneous orbital magnetic moment [52,44]. The experiments of Ref. [47] are able to scan across the critical point at $s = 0$, and observe behavior consistent with (58); we regard this as strong evidence for the phase diagram of Fig 13 with a quantum critical point between $d_{x^2-y^2}$ and $d_{x^2-y^2} + id_{xy}$ superconductors. It would be interesting if future experiments are able to test for the corrections to (58) discussed in Section 6.2. We also note here the recent measurements of Yeh *et al.* [53] presenting evidence for related (but somewhat different) changes in the pairing symmetry in the overdoped regime.

7 Conclusions

We have studied a number of phase transitions of two dimensional correlated electron systems and a schematic phase diagram summarizing their relevance to the high temperature superconductors was in Fig 13. At zero doping, $\delta = 0$, we start from an insulating antiferromagnet with long range Néel order. After a localized carrier regime at very low doping, the ground state at small δ appears to be superconducting with co-existing collinear spin-density wave order (the SC+SDW phase). There is a long in-plane spin correlation length in this phase (the finiteness of the correlation length is, we believe, due to disorder effects, and so at long enough scales the spin order is spin-glass like). At special commensurate dopings (like $\delta = 1/8$) the inter-plane coupling is strong enough to induce three-dimensional long-range order at finite temperatures.

At larger δ there is a transition to a pure $d_{x^2-y^2}$ superconductor, and this transition was described in Section 5. Charge order and its fluctuations also play a central role in the magnetic ordering quantum transition: we discussed these effects in the insulator in Section 4. They also have an important effect near the corresponding SC+SDW to SC transition in the superconductor, but the reader is referred to [21] for a review of these.

With increasing δ, we argued on the basis of theoretical [41,42] and experimental studies [47] that the cuprate superconductors are at least in the vicinity of a separate transition from the $d_{x^2-y^2}$ superconductor to a $d_{x^2-y^2} + id_{xy}$ superconductor. A quantum field theory for this transition, associated with the breakdown of BCS theory at the critical point, was presented in Section 6.

Acknowledgements

References

[1] S. Sachdev, *Quantum Phase Transitions*, Cambridge University Press, Cambridge (1999).

[2] S. Sachdev, Science, **288**, 475 (2000).

[3] M. Azuma, Z. Hiroi, M. Takano, K. Ishida, and Y. Kitaoka Phys. Rev. Lett. **73**, 3463 (1994).

[4] E. Dagotto and T. M. Rice, Science **271**, 618 (1996).

[5] N. Katoh and M. Imada, J. Phys. Soc. Jpn. **63**, 4529 (1994).

[6] J. Tworzydlo, O. Y. Osman, C. N. A. van Duin, and J. Zaanen, Phys. Rev. B **59**, 115 (1999).

[7] M. Matsumoto, C. Yasuda, S. Todo, and H. Takayama, cond-mat/0107115.

[8] S. Sachdev and K. Park, cond-mat/0108214.

[9] F. D. M. Haldane, Phys. Rev. B **25**, 4925 (1982).

[10] N. Read and S. Sachdev, Phys. Rev. Lett. **62**, 1694 (1989).

[11] N. Read and S. Sachdev, Phys. Rev. B **42**, 4568 (1990).

[12] E. Fradkin and S. A. Kivelson, Mod. Phys. Lett. B **4**, 225 (1990).

[13] W. Zheng and S. Sachdev, Phys. Rev. B **40**, 2704 (1989).

[14] I. Affleck, T. Kennedy, E. H. Lieb, and H. Tasaki, Phys. Rev. Lett. **59**, 799 (1987).

[15] O. P. Sushkov, J. Oitmaa, and Zheng Weihong, Phys. Rev. B **63**, 104420 (2001).

[16] M. S. L. du Croo de Jongh, J. M. J. van Leeuwen, W. van Saarloos, Phys. Rev. B **62**, 14844 (2000).

[17] D. Rokhsar and S. A. Kivelson, Phys. Rev. Lett. **61**, 2376 (1988)

[18] R. Moessner and S. L. Sondhi, Phys. Rev. Lett. **86**, 1881 (2001).

[19] S. Sachdev and N. Read, Phys. Rev. Lett. **77**, 4800 (1996).

[20] C. Di Castro, M. Grilli, and S. Caprara, cond-mat/0109319 and references therein.

[21] S. Sachdev, cond-mat/0108238.

[22] L. Balents, M. P. A. Fisher, and C. Nayak, Int. J. Mod. Phys. B **12**, 1033 (1998).

[23] S. Sachdev and J. Ye, Phys. Rev. Lett. **69**, 2411 (1992).

[24] A. V. Chubukov, S. Sachdev, and J. Ye, Phys. Rev. B **49**, 11919 (1994).

[25] J. Rossat-Mignod, L. P. Regnault, C. Vettier, P. Bourges, P. Burlet, J. Bossy, J. Y. Henry, and G. Lapertot, Physica C **185-189**, 86 (1991).

[26] H. A. Mook, M. Yethiraj, G. Aeppli, T. E. Mason, and T. Armstrong, Phys. Rev. Lett. **70**, 3490 (1993).

[27] H. F. Fong, B. Keimer, D. Reznik, D. L. Milius, and I. A. Aksay, Phys. Rev. B **54**, 6708 (1996).

[28] H. F. Fong, B. Keimer, D. L. Milius, and I. A. Aksay, Phys. Rev. Lett. **78**, 713 (1997).

[29] P. Bourges in *The Gap Symmetry and Fluctuations in High Temperature Superconductors* ed. J. Bok, G. Deutscher, D. Pavuna, and S. A. Wolf (Plenum, New York, 1998), cond-mat/9901333.

[30] S. Sachdev, C. Buragohain, and M. Vojta, Science **286**, 2479 (1999).

[31] M. Vojta, C. Buragohain, and S. Sachdev, Phys. Rev. B **61**, 15152 (2000).

[32] E. Demler, S. Sachdev, and Y. Zhang, Phys. Rev. Lett. **87**, 067202 (2001).

[33] H. F. Fong, P. Bourges, Y. Sidis, L. P. Regnault, J. Bossy, A. Ivanov, D. L. Milius, I. A. Aksay, and B. Keimer, Phys. Rev. Lett. **82**, 1939 (1999).

[34] Y. Sidis, P. Bourges, H. F. Fong, B. Keimer, L. P. Regnault, J. Bossy, A. Ivanov, B. Hennion, P. Gautier-Picard, G. Collin, D. L. Millius, and I. A. Aksay, Phys. Rev. Lett. **84**, 5900 (2000).

[35] B. Khaykovich, Y. S. Lee, S. Wakimoto, K. J. Thomas, R. Erwin, S.-H. Lee, M. A. Kastner, and R. J. Birgeneau, preprint.

[36] B. Lake, G. Aeppli, K. N. Clausen, D. F. McMorrow, K. Lefmann, N. E. Hussey, N. Mangkorntong, M. Nohara, H. Takagi, T. E. Mason, and A. Schröder, Science **291**, 1759 (2001).

[37] T. Valla, A. V. Fedorov, P. D. Johnson, B. O. Wells, S. L. Hulbert, Q. Li, G. D. Gu, and N. Koshizuka, Science **285**, 2110 (1999).

[38] M. Vojta, Y. Zhang, and S. Sachdev, Phys. Rev. B **62**, 6721 (2000).

[39] M. Vojta, Y. Zhang, and S. Sachdev, Phys. Rev. Lett. **85**, 4940 (2000).

[40] C. J. Halboth and W. Metzner Phys. Rev. Lett. **85**, 5162 (2000).

[41] M. A. Baranov and M. Yu Kagan, Z. Phys. B **86**, 237 (1992).

[42] M. A. Baranov, A. V. Chubukov, and M. Yu Kagan, Int. J. Mod. Phys. B **6**, 2471 (1992).

[43] R. B. Laughlin, Phys. Rev. Lett. **80**, 5188 (1998).

[44] M.-R. Li, P. J. Hirschfeld, and P. Woelfle, Phys. Rev. B **63**, 054504 (2001).

[45] K. Park and S. Sachdev, Phys. Rev. B in press, cond-mat/0104519.

[46] M. Granath, V. Oganesyan, S. A. Kivelson, E. Fradkin, and V. J. Emery, cond-mat/0010350.

[47] Y. Dagan and G. Deutscher, Phys. Rev. Lett. in press, cond-mat/0106128.

[48] M. Vojta, Y. Zhang, and S. Sachdev, Int. J. Mod. Phys. B **14**, 3719 (2000); cond-mat/0008048.

[49] D. V. Khveshchenko and J. Paaske, Phys. Rev. Lett. **86**, 4672 (2001).

[50] B. Rosenstein, B. J. Warr, and S. H. Park, Phys. Rep. **205**, 59 (1991).

[51] L. Kärkkäinen, R. Lacaze, P. Lacock, and B. Petersson, Nucl. Phys. B **415**, 781 (1994).

[52] T. Koyama and M. Tachiki, Phys. Rev. B **53**, 2662 (1996).

[53] N.-C. Yeh, C.-T. Chen, G. Hammerl, J. Mannhart, A. Schmehl, C. W. Schneider, R. R. Schulz, S. Tajima, K. Yoshida, D. Garrigus, and M. Strasik, Phys. Rev. Lett. **87**, 087003 (2001).